Norbornadiene photoswitches anchored to well-defined oxide surfaces: From ultrahigh vacuum into the liquid and the electrochemical

The Journal of Chemical Physics

Norbornadiene photoswitches anchored to well-defined oxide surfaces: From ultrahigh vacuum into the liquid and the electrochemical environment

Cite as: J. Chem. Phys. **152**, 044708 (2020); https://doi.org/10.1063/1.5137897
Submitted: 13 November 2019 . Accepted: 15 December 2019 . Published Online: 23 January 2020

Manon Bertram, Fabian Waidhas, Martyn Jevric, Lukas Fromm, Christian Schuschke, Maximilian Kastenmeier, Andreas Görling, Kasper Moth-Poulsen, Olaf Brummel, and Jörg Libuda

The Journal of Chemical Physics ARTICLE scitation.org/journal/jcp

Norbornadiene photoswitches anchored to well-defined oxide surfaces: From ultrahigh vacuum into the liquid and the electrochemical environment

Cite as: J. Chem. Phys. 152, 044708 (2020); doi: 10.1063/1.5137897
Submitted: 13 November 2019 • Accepted: 15 December 2019 •
Published Online: 23 January 2020

Manon Bertram,[1] Fabian Waidhas,[1] Martyn Jevric,[2] Lukas Fromm,[3] Christian Schuschke,[1] Maximilian Kastenmeier,[1] Andreas Görling,[3] Kasper Moth-Poulsen,[2] Olaf Brummel,[1,a)] and Jörg Libuda[1]

AFFILIATIONS

[1]Interface Research and Catalysis, Erlangen Catalysis Resource Center, Friedrich-Alexander-Universität Erlangen-Nürnberg, Egerlandstraße 3, 91058 Erlangen, Germany
[2]Department of Chemistry and Chemical Engineering, Chalmers University of Technology, 41296 Gothenburg, Sweden
[3]Lehrstuhl für Theoretische Chemie, Friedrich-Alexander-Universität Erlangen-Nürnberg, Egerlandstraße 3, 91058 Erlangen, Germany

Note: This article is part of the JCP Special Topic on Oxide Chemistry and Catalysis.
[a)]**Author to whom correspondence should be addressed:** olaf.brummel@fau.de

ABSTRACT

Employing molecular photoswitches, we can combine solar energy conversion, storage, and release in an extremely simple single molecule system. In order to release the stored energy as electricity, the photoswitch has to interact with a semiconducting electrode surface. In this work, we explore a solar-energy-storing model system, consisting of a molecular photoswitch anchored to an atomically defined oxide surface in a liquid electrolyte and under potential control. Previously, this model system has been proven to be operational under ultrahigh vacuum (UHV) conditions. We used the tailor-made norbornadiene derivative 2-cyano-3-(4-carboxyphenyl)norbornadiene (CNBD) and characterized its photochemical and electrochemical properties in an organic electrolyte. Next, we assembled a monolayer of CNBD on a well-ordered $Co_3O_4(111)$ surface by physical vapor deposition in UHV. This model interface was then transferred into the liquid electrolyte and investigated by photoelectrochemical infrared reflection absorption spectroscopy experiments. We demonstrate that the anchored monolayer of CNBD can be converted photochemically to its energy-rich counterpart 2-cyano-3-(4-carboxyphenyl)quadricyclane (CQC) under potential control. However, the reconversion potential of anchored CQC overlaps with the oxidation and decomposition potential of CNBD, which limits the electrochemically triggered reconversion.

INTRODUCTION

Solar energy conversion and storage are of central interest in the transition toward a renewable energy system.[1] Here, molecular photoswitches provide a straightforward chemical method to store solar energy at large time scales.[2–5] Moreover, molecular photoswitches are an exceptionally simple alternative to conventional photovoltaic technologies. Among the different photoswitches, the valence couple norbornadiene (NBD)/quadricyclane (QC) is a prominent example[6–9] that has recently received renewed attention.[10–16] In this storage couple, the energy-lean NBD is converted photochemically to its metastable and energy-rich

isomer QC via an intramolecular cycloaddition. During this process, up to 100 kJ/mol of chemical energy is stored, a value comparable to state-of-the-art batteries.[17,18]

In current research, several challenges were tackled successfully that impede the use of the NBD-QC system in solar-energy harvesting.[19–22] Pristine NBD adsorbs light at wavelengths below 300 nm only. Therefore, photosensitizers are required to initiate the conversion.[23–25] Photosensitizers, however, reduce the stability of QC and cause degradation during the catalytically triggered energy release.[25] Precise molecular design addressed these issues: Substituted NBD-derivatives were synthesized that combine beneficial absorption properties with a low molecular weight.[26] Additional advances in molecular design circumvent the possible destabilization of QC isomers caused by red-shifting the absorption maximum of the NBD unit.[27,28]

Further challenges are encountered during the catalytically triggered energy release process. Typically, this process is initiated by adding homogeneous, mildly oxidizing agents.[29–31] Homogeneous catalysts, however, provide a low level of control and may cause additional stability issues. Therefore, heterogeneous catalysts are preferred.[13,15,20,32] For example, this approach has been recently demonstrated in a molecular solar thermal (MOST) storage device for solution based NBD, which releases macroscopic heat catalytically at a carbon-supported cobalt phthalocyanine interface.[20]

Another particularly intriguing concept is to release the energy stored in the NBD/QC-system electrochemically. Recently, we have shown that the reconversion can, indeed, be controlled by an applied potential.[25,33,34] In combination with the molecular design, a reversibility of more than 99% per cycle was achieved in the electrochemically triggered energy storage system.[34] Photochemical conversion and electrochemically triggered energy release were monitored *in situ* in a specifically developed experimental setup.[25]

Based on these achievements, we envision that it might be possible to release the energy stored in the NBD photoswitch directly in the form of electricity, in a concept inspired by dye sensitized solar cells.[33] In the classical dye sensitized solar cell, a semiconducting electrode is functionalized with the dye via suitable anchor groups.[35] Similarly, here, we aim to anchor a functional photoswitch to a semiconducting electrode.

In recent studies, we demonstrated that the use of well-defined oxide surfaces enables investigating the adsorption properties of organic molecules with specific anchor groups and their binding motives both in ultrahigh vacuum (UHV)[36,37] and in electrochemical environments.[38] In our latest research, we have reported on a functional energy storing hybrid interface, using such a well-defined oxide surface.[39] We prepared a photoswitchable NBD monolayer anchored to an atomically defined cobalt oxide surface under ultraclean conditions in UHV. The NBD derivative comprises an extended conjugation through a 2,3-olefin to red-shift the absorption maximum, a spectroscopic marker that enables monitoring of the conversion by *in situ* IR spectroscopy, and a carboxylic acid linker group for anchoring at the oxide surface. The oxide, an atomically defined $Co_3O_4(111)$ film, has a well-known surface structure.[40] Employing this model system, photoswitching and thermally triggered energy release were achieved with high reversibility under UHV conditions.[39]

In this work, we go one step further. We employ the same model system, prepared in UHV, and transfer it into an electrochemical environment without exposure to ambient conditions. We demonstrate that a single monolayer of the NBD derivative anchored to the $Co_3O_4(111)$ surface remains intact upon transfer into the liquid environment and can be photoconverted to its QC counterpart.

EXPERIMENTAL

Experimental setup

All samples were prepared at a UHV setup consisting of a preparation chamber and a dedicated transfer system. Details of the setup can be found elsewhere.[41]

Preparation of the $Co_3O_4(111)$ film

The $Co_3O_4(111)$ thin films were prepared on an Ir(100) single crystal (MaTeck, 99.99%, depth of roughness <0.01 μm, accuracy of orientation <0.1°) employing an adapted method based on the procedure of Heinz and Hammer.[40,42] The crystal was cleaned by Ar^+ bombardment (Linde 6.0, 9×10^{-5} mbar, 1.8 keV, 300 K) and annealing cycles (UHV, 1123 K, 5 min; followed by annealing in O_2, Linde 5.0, 5×10^{-8} mbar, 1123 K). The Ir(100)-(5×1) reconstructed surface was obtained by flashing the sample to 1123 K in UHV. Successive flashing of the surface to 873 K in O_2 atmosphere (5×10^{-8} mbar) and cooling to 393 K in O_2 yielded the Ir(100)-(2×1)O reconstruction as confirmed by LEED. Cobalt (Alfa Aesar, 99.95%, 2 mm rod) was deposited in a reactive O_2 atmosphere (8×10^{-6} mbar) at temperatures between 300 and 243 K to avoid an initial adsorption of water. The Co evaporation rate was calibrated by a quartz crystal microbalance and the evaporation time adjusted to give films of 6 nm thickness. An ordered film was formed by annealing in O_2 (5×10^{-7} mbar) at 523 K for 3 min, at 698 K for 5 min (1×10^{-7} mbar), and subsequent annealing in UHV at 698 K for 3 min, as confirmed by LEED.

PVD of CNBD

2-cyano-3-(4-carboxyphenyl)norbornadiene (CNBD) was evaporated from a glass crucible employing a home-built Knudsen cell evaporator mounted to a translation stage. Prior to the first experiment, the evaporator was baked for 24 h while being separated from the main chamber by a gate valve and being pumped by a separate high vacuum line. Before deposition, the evaporator was preheated to 370 K before the gate valve was opened and the evaporator moved into the chamber. CNBD was deposited at a sample temperature of 300 K.

Transfer

For photoconversion and spectroelectrochemical analysis, the CNBD-$Co_3O_4(111)$ samples were transferred out of the UHV chamber following a procedure described in detail elsewhere.[41,43] In brief, after decoupling the transfer stage and electrochemical transfer cell from the preparation chamber, the former were purged with N_2 (Linde 5.0). The crystal was removed from its holder and the cell

detached from the transfer stage and sealed for transport in N_2 atmosphere while continuously flowing N_2.

Cleaning of the electrochemical equipment

All glass ware, Teflon parts, and noble metal wires employed in the electrochemical measurements were stored in sulfuric acid (98%, Merck, EMSURE) containing NOCHROMIX (Sigma Aldrich). Before use, the equipment was first rinsed with ultrapure water (MilliQ synergy UV, 18.2 MΩ cm at 25 °C, < 5 ppb total organic carbon) five times and then boiled in ultrapure water three times. Finally, the equipment was dried under vacuum overnight.

PEC-IRRAS

The photoelectrochemical infrared reflection absorption spectroscopy (PEC-IRRAS) experiments were conducted with a vacuum-based FT-IR spectrometer (Bruker Vertex 80v) with evacuated optics, IR optics for electrochemical measurements (Bruker), and a liquid-nitrogen-cooled narrow band mercury-cadmium-telluride detector. For the photochemical experiments, the spectrometer was further equipped with a high-power UV light-emitting diode (LED) (Seoul Viosys, CUN6AF4A, 365 nm, 2.35 W) located underneath a CaF_2 hemisphere (Korth, diameter 25 mm), which served as IR and UV transparent window. A detailed description of the setup is reported in our previous work.[25] All spectra are obtained in reflection mode and thin layer configuration.

The UHV-prepared samples were attached to a Pt wire (Hauner, 99.95%) in a protective N_2 atmosphere (Linde, 5.0). Experiments without external potential applied were conducted in dichloromethane (DCM) (Sigma-Aldrich, ≥99.8%), while electrochemically controlled experiments were performed in 0.1M tetrabutylammonium perchlorate (Sigma Aldrich, 99.0%) in DCM. The potential was controlled by a commercial potentiostat (Gamry Reference 600) operated by the Framework software. A graphite rod served as counter electrode (CE), while a saturated Ag/Ag^+ electrode ($AgNO_3$ with 0.1M tetrabutylammonium perchlorate in DCM) was used as reference electrode (RE). The reference electrode was calibrated by recording cyclic voltammograms of 10 mM ferrocene (Alfa Aesar, 99.5%) in DCM in a separate cell prior to and after each measurement. Accordingly, all potentials in this work are referred to ferrocene (V_{fc}). The UHV-prepared thin films served as the working electrode.

All spectra were acquired with a spectral resolution of 2 cm^{-1}. Spectra of the UHV-prepared CNBD monolayer were recorded with an acquisition time of 4 min (512 scans). A background spectrum was taken with an acquisition time of 8 min (1024 scans). For spectra recorded in a 10 mM CNBD solution at a pristine $Co_3O_4(111)$ thin film, the acquisition time was reduced to 57 s (128 scans) and 4 min (512 scans) for the background spectrum, respectively.

DFT calculations

Density functional theory (DFT) calculations were performed with the TURBOMOLE package v7.2[44] with the conductor-like screening model COSMO to take the solvent effects into account. The exchange-correlation was modeled with the Perdew-Burke-Ernzerhof functional[45] using the def2-TZVP basis set by Weigend and Ahlrichs.[46] The D3 dispersion correction[47] with a Becke-Johnson damping[48] was applied to mimic long-range van-der-Waals interactions. To accelerate the calculation, the RI-J approximation was applied.[49] Vibrational spectra were calculated within the harmonic approximation.

Synthesis

CNBD was synthesized in a multistep sequence. Starting from the commercially available 4-iodoacetophenone, the respective propiolonitrile was yielded after a three-step transformation of the acetyl functionality. A Diels-Alder [4 + 2π] cycloaddition at the acetylene moiety with cyclopentadiene resulted in the formation of 3-(4-iodophenyl)norbornadiene-2-carbonitrile. An iodine-magnesium exchange was promoted by applying Knöchel conditions. Finally, trapping the carbanion with carbon dioxide yielded CNBD. All intermediates and products were characterized by ^1H NMR and ^{13}C NMR. The final products were further characterized by various techniques (UV-Vis spectroscopy, differential scanning calorimetry, and single-crystal X-ray crystal structural analysis). For details of the synthesis and results of the characterization, we refer to Ref. 39.

RESULTS AND DISCUSSION

Photoelectrochemistry in solution

In the first step, we tested the photochemical and electrochemical behavior of the NBD derivative 2-cyano-3-(4-carboxyphenyl) norbornadiene (CNBD) in solution. The molecule, which was later also used to prepare the hybrid interface, is shown in Fig. 1(a). For information on synthesis and properties, we refer to Ref. 39. The molecule consists of structural units providing four functionalities: (i) the NBD storage unit, (ii) an extended conjugation via the 2,3-olefin red-shifting the light absorption region, (iii) the CN group also acting as spectroscopic marker, and (iv) the carboxylate group serving as an anchor to the oxide surface. CNBD features an absorption onset at 378 nm and an absorption maximum at 319 nm.[39] Upon irradiation in the UV region, the energy lean CNBD is photoconverted to its energy-rich counterpart CQC.

We investigated the photo- and electrochemical properties of CNBD/CQC in solution using an electrode consisting of an ordered $Co_3O_4(111)$ film prepared on an Ir(100) single crystal surface (see the section titled "Experimental" for details). We performed photoelectrochemical infrared reflection absorption spectroscopy (PEC-IRRAS)[25] in a 10 mM solution of CNBD in DCM with 0.1M tetrabutylammonium perchlorate as the supporting electrolyte. The experimental procedure is illustrated in Fig. 1(b). In our previous study, we used the same procedure to investigate the photochemical and electrochemical conversion of 2-cyano-3-(3,4-dimethoxyphenyl)-norbornadiene/quadricyclane.[34] First, we applied a potential of −0.88 V_{fc} and recorded a reference spectrum. After irradiating the sample with a UV pulse (365 nm, 2.35 W, 5 s), we acquired another spectrum and increased the potential in 0.1 V steps up to 1.82 V_{fc} recording an additional spectrum at every step (see Ref. 25 for details of the experimental setup).

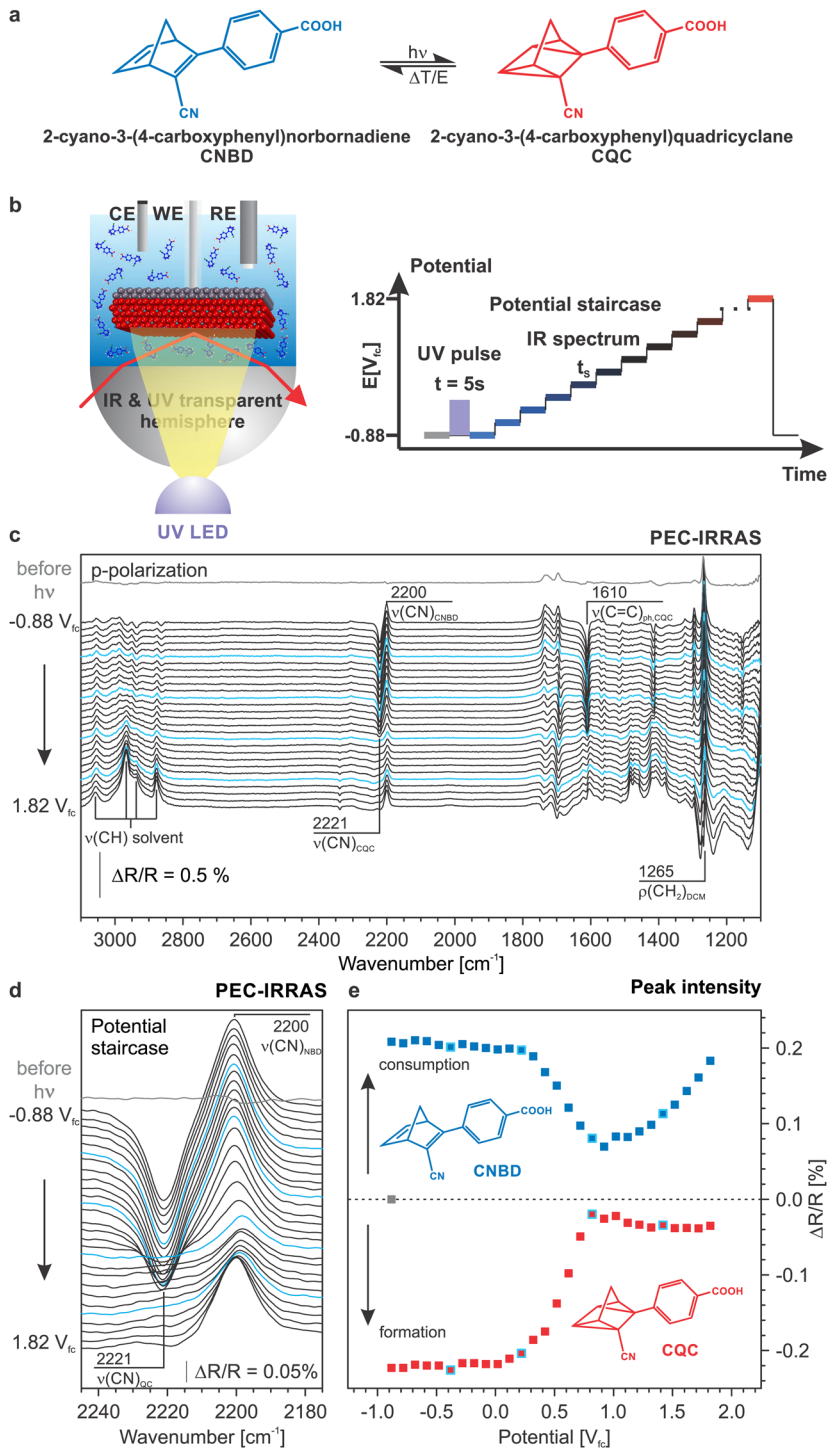

FIG. 1. PEC-IRRAS of CNBD in solution. (a) Molecular structures of the isomer couple CNBD/CQC. (b) Scheme of the experimental procedure for PEC-IRRAS. (c) PEC-IRRAS spectra of 10 mM CNBD at a UHV-prepared $Co_3O_4(111)$ surface in 0.1M tetrabutylammonium perchlorate in DCM. (d) Zoom into the CN stretching region. (e) Peak intensities for the ν(CN) band of CNBD (blue) and CQC (red) as a function of the potential.

The results are displayed in Fig. 1(c). Note that all spectra are presented as difference spectra using the background taken before irradiation as reference. Positive bands, therefore, correspond to species consumed, while negative bands correspond to species which are formed (with respect to the reference). In Fig. 1(c), only the most prominent vibrational bands are marked. A complete assignment based on density functional theory (DFT) is given in Chapter 1 of the Supplementary Material. The most important feature in this

work is the CN stretching vibration ν(CN) [Fig. 1(d)], which enables us to differentiate between CNBD and CQC. The positive band at 2200 cm^{-1} is assigned to the CN stretching vibration $\nu(CN)_{CNBD}$ of CNBD (DFT 2198 cm^{-1}) and the blue-shifted, negative band at 2221 cm^{-1} is assigned to the stretching vibration $\nu(CN)_{CQC}$ of CQC (DFT 2223 cm^{-1}). The appearance of both bands indicates conversion of CNBD to CQC upon irradiation. Additional strong bands after irradiation at 1610 cm^{-1} (negative) and 1265 cm^{-1} (positive) correspond to a C=C stretching vibration, $\nu(C{=}C)_{phenyl,CQC}$, of the phenyl ring in CQC and the HCH wagging mode, $\omega(CH_2)_{DCM}$, of the solvent DCM, respectively.[50] After increasing the potential, further strong positive bands above 2800 cm^{-1} are assigned to the symmetric and antisymmetric CH stretching modes ν(CH) arising from DCM and the tetrabutylammonium entity.

Figure 1(e) illustrates the intensity of the $\nu(CN)_{CNBD}$ (upper half) and the $\nu(CN)_{CQC}$ (lower half) bands dependent on the potential applied. With increasing potential, the positive $\nu(CN)_{CNBD}$ and the negative $\nu(CN)_{CQC}$ bands start to decrease at 0.12 V_{fc}. At 0.82 V_{fc}, the negative CQC vibration has vanished, while the $\nu(CN)_{CNBD}$ band starts to increase again. The concomitant loss of peak intensity for both species in the intermediate potential range indicates that CQC is consumed, while CNBD is formed, i.e., CQC is reconverted to CNBD.

We assign the increasing $\nu(CN)_{CNBD}$ at higher potentials to the oxidation of CNBD. The onset potential for the decomposition of CNBD is overlapping with the region of reconversion. This is in sharp contrast to our previous study of 2-cyano-3-(3,4-dimethoxyphenyl)-norbornadiene and its quadricyclane counterpart,[34] where we could clearly separate reconversion and decomposition (onset 0.9 V_{fc}). The onset potential for the decomposition of CNBD is shifted to lower potentials as compared to 2-cyano-3-(3,4-dimethoxyphenyl)-norbornadiene. We attribute this effect to the influence of the substituents on the aromatic ring.

In order to further analyze the oxidation or decomposition reactions accompanying the incomplete reconversion from CQC to CNBD, DFT calculations were performed on band positions of possible decomposition products and the results were compared to the experimental data. Calculations and comparisons are presented in Chapter 1 of the Supplementary Material. Briefly, many of the potential decomposition products feature similar band positions. Therefore, a more detailed identification of the decomposition products is not possible based only on the IR spectroscopic data.

Photochemistry in the monolayer

In the next step, we investigated the photochemical behavior of the anchored CNBD monolayer in solution. The experimental procedure is presented in Fig. 2(a). The CNBD monolayer was prepared by physical vapor deposition (PVD) onto a freshly prepared $Co_3O_4(111)$ thin film held at a sample temperature of 300 K. Note that CNBD can be evaporated without decomposition and that the CNBD multilayer desorption temperature is at 280 K.[39] Therefore, PVD at a sample temperature of 300 K leads to the formation of

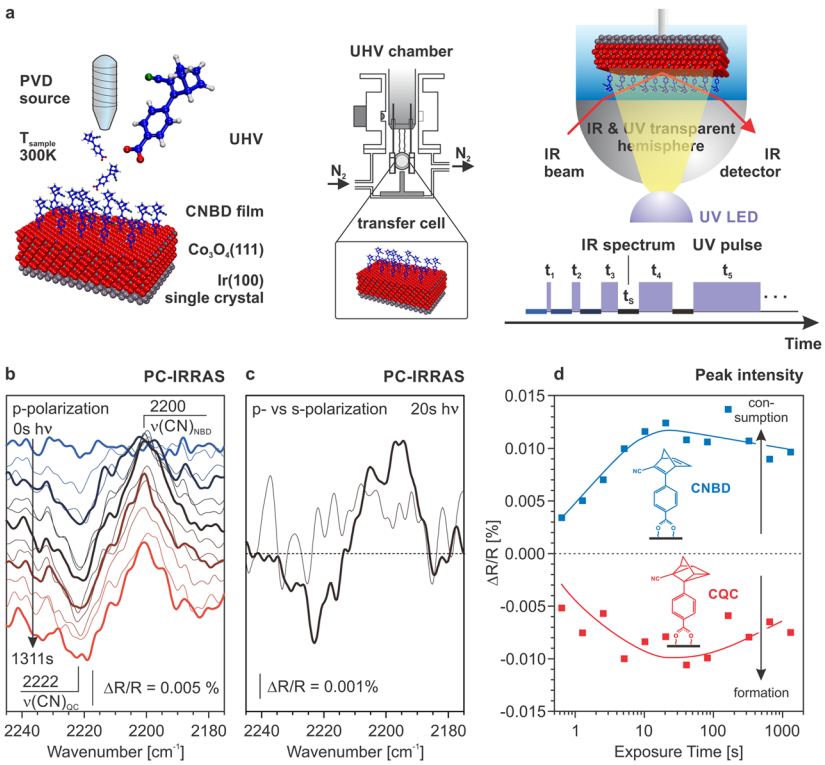

FIG. 2. Photochemistry of the CNBD monolayer anchored to $Co_3O_4(111)$ in solution (DCM). (a) Experimental procedure including sample preparation in UHV, transfer into the liquid environment, and description of the measurement protocol applied. (b) CN stretching region depicting IR spectra in p-polarization recorded after UV irradiation. (c) Comparison of the IR spectra obtained after a total UV exposure time of 20 s acquired in p-polarization (thick lines) and in s-polarization (thin lines). (d) ν(CN) peak intensities after UV exposure for CNBD (blue) and CQC (red) as a function of the irradiation time.

an anchored monolayer only. After preparation of the monolayer film, the sample was transferred from UHV into the liquid environment under clean conditions, i.e., without exposure to ambient conditions. Details on the experimental setup and procedure were reported previously.[41]

In the first set of experiments, we used pure DCM as a solvent and did not apply any external potential. These experiments were performed to test whether the anchored monolayer film is stable in DCM and whether it can be photochemically converted to CQC. We performed a set of photochemical IRRAS (PC-IRRAS) experiments, i.e., we exposed the CNBD monolayer to exponentially increasing doses of UV light (total irradiation times of 0.64, 1.28, 2.56, 5.12, 10.24, 20.48, 40.96, 81.92, 163.8, 327.7, 655.4, and 1311 s) and recorded a spectrum after each UV pulse. All IR spectra were acquired in p-polarization (which is sensitive to species at the electrode/solvent interface). Figure 2(b) depicts the CN stretching region for these experiments. The complete spectral range is provided in Chapter 2 of the Supplementary Material.

With an increasing UV exposure time, a positive $\nu(CN)_{CNBD}$ band develops at 2200 cm^{-1}, while a negative $\nu(CN)_{CQC}$ band

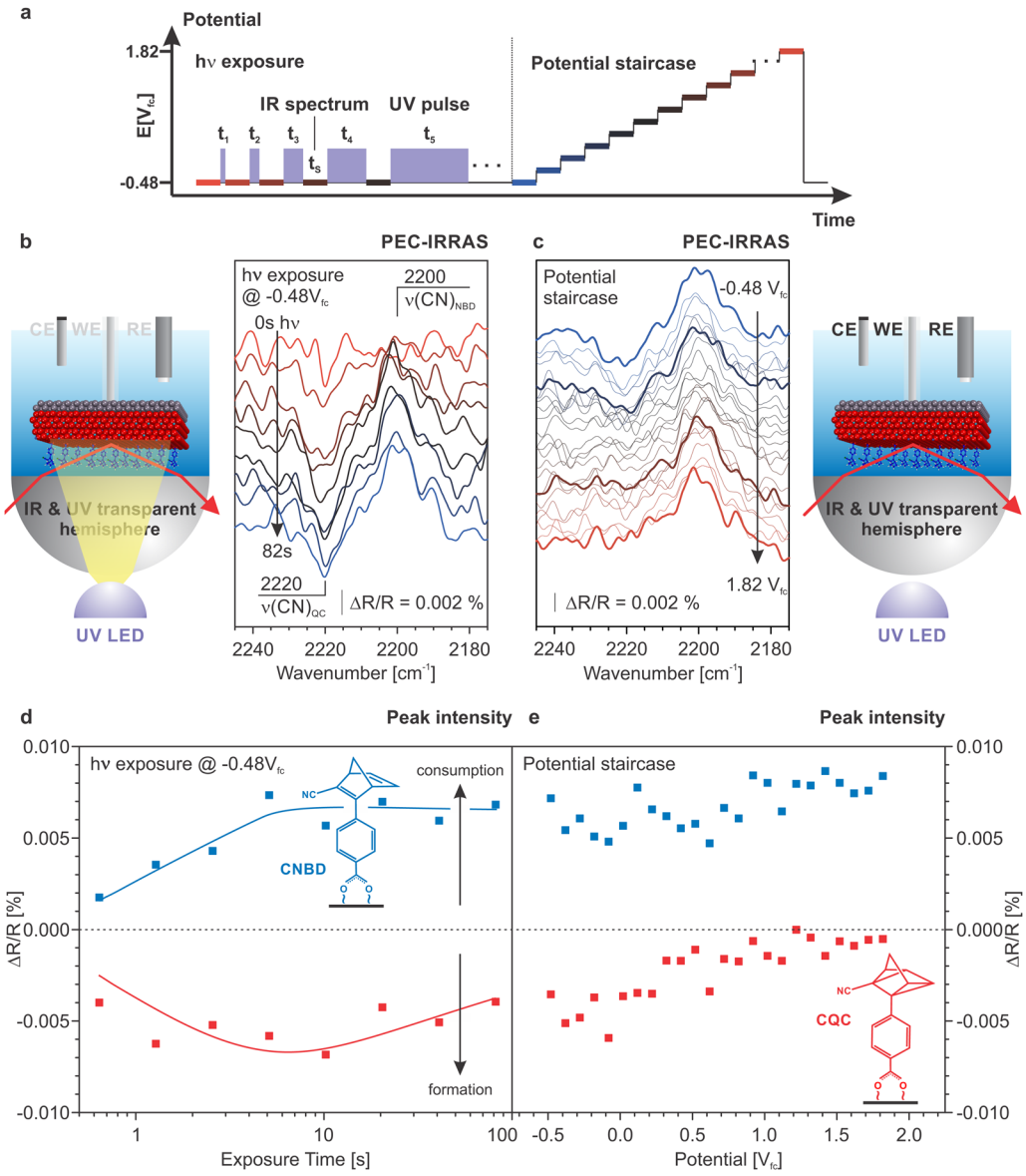

FIG. 3. Photoelectrochemistry of the CNBD monolayer anchored to $Co_3O_4(111)$ in solution (0.1M tetrabutylammonium perchlorate in DCM). (a) Experimental procedure involving UV exposure at −0.48 V_{fc} and potential staircase up to 1.82 V_{fc}. (b) and (c) IR spectra in the CN stretching region (p-polarization) recorded after UV irradiation and potential staircase. (d) and (e) Peak intensities of ν(CN) band after UV exposure and potential staircase for CNBD (blue) and CQC (red).

forms at 2222 cm^{-1}. This observation indicates that indeed the anchored CNBD is photochemically converted to CQC. To determine if unconverted CNBD remains adsorbed on the $Co_3O_4(111)$ surface, we exposed a CNBD monolayer to 20 s of UV light and recorded spectra in both, p- and s-polarization. Note that species in solution are observable both in p- and in s-polarization, whereas species adsorbed on the surface, due to the metal surface selection rule, are detectable in p-polarization only.[51] The results are displayed in Fig. 2(c). While the typical bands of CNBD and CQC are recorded in the CN stretching region with p-polarized light, no bands are observed in s-polarization. This clearly demonstrates that the CNBD monolayer remains intact in solution and that the photochemical reaction takes place at the solvent/oxide interface. Note further that the CN band intensity is in the same order of magnitude as observed for conversion in UHV.[39] This underlines the stability of the monolayer upon transfer to solution.

In Fig. 2(d), the peak intensities are depicted of CNBD (upper half, blue) and CQC (lower half, red) as a function of exposure time. The data was obtained from the spectra in Fig. 2(b). At low UV exposure, the peak intensities increase nearly linearly. At exposure times of around 30 s, the conversion levels off. A slight drop of the CQC band is observable upon extended UV exposure (>100 s).

The rapidly increasing peak intensities of CNBD and CQC demonstrate that the anchored CNBD monolayer is converted to CQC in the liquid environment. Assuming a full conversion of the monolayer after 30 s of UV exposure yields an external quantum efficiency of 7×10^{-6}.[25,39] The slight drop in the peak intensity at long exposure times is attributed to the photochemically induced decomposition of the molecules and to thermally activated reconversion. Note that prolonged UV exposure with the high power LED can heat up the experimental setup, resulting in faster thermally activated reconversion (see Ref. 39 for details).

Photoelectrochemistry in the monolayer

Finally, we probe the photochemical conversion of the CNBD monolayer anchored to the $Co_3O_4(111)$ surface under potential control. To this end, a CNBD monolayer was evaporated onto a freshly prepared $Co_3O_4(111)$ film and the sample transferred out of UHV into the electrolyte as described in this section and the Experimental section. Subsequently, PEC-IRRAS measurements were performed following the procedure depicted in Fig. 3(a). The sample was immersed into a solution of 0.1M tetrabutylammonium perchlorate in DCM under potential control at −0.48 V_{fc}. Note that at an electrode potential of −0.48 V_{fc}, no reconversion was observed for photoconverted CQC in solution (see above). At this potential, the CNBD monolayer was exposed to exponentially increasing doses of UV light (total irradiation times of 0.64, 1.28, 2.56, 5.12, 10.24, 20.48, 40.96, and 81.92 s) while recording spectra after each pulse. After UV exposure, the potential was ramped to 1.82 V_{fc} in steps of 0.1 V, and an IR spectrum was acquired after each potential step. All spectra were acquired in p-polarization. In Fig. 3(b), the CN stretching region is displayed for spectra recorded after each individual UV exposure. In Fig. 3(c), we display the CN stretching region recorded while ramping the potential. The corresponding maximum peak intensities are illustrated in Figs. 3(d) and 3(e), respectively. The full spectral range is provided in Chapter 2 of the Supplementary Material.

The increasing positive band at 2200 cm^{-1} (indicating consumption of CNBD) and the negative band developing at 2220 cm^{-1} (indicating formation of CQC) during UV exposure reveal that the CNBD monolayer is successfully converted to CQC under potential control. Upon increasing the electrode potential, the negative $\nu(CN)_{CQC}$ band at 2220 cm^{-1} decreases, starting at 0.02 V_{fc}. At ~0.72 V_{fc}, the $\nu(CN)_{CQC}$ band has vanished completely. While the $\nu(CN)_{CQC}$ band decreases, however, the intensity of the $\nu(CN)_{CNBD}$ at 2200 cm^{-1} stays approximately constant. This observation indicates that the CQC in the anchored monolayer is consumed, but the reaction does not lead to the formation of anchored CNBD again. We attribute this effect to the irreversible electro-oxidation of the surface-bound photoswitch. This oxidation occurs at potentials, which overlap with the potential of the reconversion. Potential oxidation reactions may involve the degradation of the conjugated π-system or may result in a modification of functional groups, i.e., of either the nitrile or the carboxylic acid moieties. Furthermore, it is likely that the anchored species undergo fragmentation and the NBD unit is detached from the surface. Due to the very strong IR bands of the solvent, however, it is difficult to identify the decomposition products by *in situ* electrochemical IR spectroscopy (see Chapter 2 of the Supplementary Material). We conclude that the CNBD/CQC photoswitch remains functional upon anchoring to the oxide surface. However, the electrochemically triggered reconversion of the anchored species would require anchoring units, which are more resistant toward oxidation than the one used in the present case.

CONCLUSION

We investigated a solar energy storing organic/oxide hybrid interface, comprising a tailor-made photoswitch, which was anchored to an atomically defined oxide surface. The photoswitch 2-cyano-3-(4-carboxyphenyl)norbornadiene (CNBD) is based on the valence couple norbornadiene-quadricyclane. Using PC-IRRAS and PEC-IRRAS, we investigated the photochemical conversion and the electrochemically triggered reconversion in solution. We used an ordered $Co_3O_4(111)$ film prepared on Ir(100) as a working electrode. The main findings are summarized as follows:

1. CNBD can be converted photochemically to CQC in solution (DCM), and the reconversion can be electrochemically triggered in solution (DCM). The onset potential for the reconversion is 0.1 V_{fc}. Above 0.8 V_{fc}, we observe oxidative decomposition of CNBD.
2. We prepared an anchored monolayer of CNBD on a well-ordered $Co_3O_4(111)$ film by PVD under UHV conditions. The sample with the functionalized interface was transferred from UHV into liquid DCM without exposure to air. The functionalized interface was shown to be intact and stable after transfer (a) into DCM without potential control and (b) into DCM with 0.1M tetrabutylammonium perchlorate under potential control at −0.48 V_{fc}.
3. The anchored monolayer of CNBD on $Co_3O_4(111)$ can be converted photochemically into anchored CQC by irradiation with UV light in liquid DCM. Conversion is possible both without potential control and with potential control at −0.48 V_{fc} in 0.1M tetrabutylammonium perchlorate in DCM.

4. In the case of the CNBD/CQC system anchored to the $Co_3O_4(111)$ surface, the potential of reconversion from CQC to CNBD competes with the potential for the oxidation of the photoswitch. As a result, the anchored CNBD decomposes during the electrochemically triggered reconversion.

Our findings show that it is possible to design an NBD/QC photoswitch, surface-anchored to a semiconducting oxide surface, which remains functional both in liquid and in electrochemical environments. Electrochemically triggered reconversion should also be possible in such a system. However, the process would require the design of anchoring units that are resistant toward oxidation at the potential that is required to trigger the reconversion from QC to NBD.

SUPPLEMENTARY MATERIAL

See the Supplementary Material for the complete assignment of the IR bands based on DFT, DFT data on possible decomposition products, and the full spectral range for the P(EC)-IRRAS experiments.

ACKNOWLEDGMENTS

This project was financially supported by Deutsche Forschungsgemeinschaft (DFG). Additional support by the DFG is acknowledged through the Research Unit FOR 1878 "funCOS – Functional Molecular Structures on Complex Oxide Surfaces". Further additional support is acknowledged through the German Federal Ministry of Education and Research (BMBF, Project Combined Infrared and X-Ray Analytics of Energy Materials, CIXenergy 05K19WE1) and the Helmholtz Institute Erlangen-Nürnberg for Renewable Energy.

REFERENCES

[1] N. S. Lewis and D. G. Nocera, Proc. Natl. Acad. Sci. U. S. A. **103**, 15729 (2006).
[2] T. J. Kucharski, Y. C. Tian, S. Akbulatov, and R. Boulatov, Energy Environ. Sci. **4**, 4449 (2011).
[3] K. Moth-Poulsen, D. Coso, K. Borjesson, N. Vinokurov, S. K. Meier, A. Majumdar, K. P. C. Vollhardt, and R. A. Segalman, Energy Environ. Sci. **5**, 8534 (2012).
[4] A. Lennartson, A. Roffey, and K. Moth-Poulsen, Tetrahedron Lett. **56**, 1457 (2015).
[5] Z. H. Wang, R. Losantos, D. Sampedro, M. Morikawa, K. Börjesson, N. Kimizuka, and K. Moth-Poulsen, J. Mater. Chem. A **7**, 15042 (2019).
[6] G. W. Dauben and R. L. Cargill, Tetrahedron **15**, 197 (1961).
[7] G. S. Hammond, P. Wyatt, C. D. DeBoer, and N. J. Turro, J. Am. Chem. Soc. **86**, 2532 (1964).
[8] D. P. Schwendiman and C. Kutal, J. Am. Chem. Soc. **99**, 5677 (1977).
[9] Z. I. Yoshida, J. Photochem. **29**, 27 (1985).
[10] A. Dreos, Z. H. Wang, B. E. Tebikachew, K. Moth-Poulsen, and J. Andreasson, J. Phys. Chem. Lett. **9**, 6174 (2018).
[11] M. Quant, A. Hamrin, A. Lennartson, P. Erhart, and K. Moth-Poulsen, J. Phys. Chem. C **123**, 7081 (2019).
[12] M. Mansø, M. D. Kilde, S. K. Singh, P. Erhart, K. Moth-Poulsen, and M. B. Nielsen, Phys. Chem. Chem. Phys. **21**, 3092 (2019).
[13] U. Bauer, S. Mohr, T. Döpper, P. Bachmann, F. Späth, F. Düll, M. Schwarz, O. Brummel, L. Fromm, U. Pinkert, A. Görling, A. Hirsch, J. Bachmann, H.-P. Steinrück, J. Libuda, and C. Papp, Chem.—Eur. J. **23**, 1613 (2017).
[14] B. S. Yeo and A. T. Bell, J. Am. Chem. Soc. **133**, 5587 (2011).
[15] U. Bauer, L. Fromm, C. Weiß, F. Späth, P. Bachmann, F. Düll, J. Steinhauer, S. Matysik, A. Pominov, A. Görling, A. Hirsch, H.-P. Steinrück, and C. Papp, J. Chem. Phys. **150**, 184706 (2019).
[16] T. Luchs, P. Lorenz, and A. Hirsch, ChemPhotoChem **3**, 1 (2019).
[17] D. P. Schwendiman and C. Kutal, Inorg. Chem. **16**, 719 (1977).
[18] K. Maruyama, K. Terada, Y. Naruta, and Y. Yamamoto, Chem. Lett. **9**, 1259 (1980).
[19] E. Vessally and S. Aryana, Russ. J. Phys. Chem. A **90**, 136 (2016).
[20] Z. H. Wang, A. Roffey, R. Losantos, A. Lennartson, M. Jevric, A. U. Petersen, M. Quant, A. Dreos, X. Wen, D. Sampedro, K. Borjesson, and K. Moth-Poulsen, Energy Environ. Sci. **12**, 187 (2019).
[21] A. U. Petersen, A. I. Hofmann, M. Fillols, M. Mansø, M. Jevric, Z. H. Wang, C. Sumby, C. Müller, and K. Moth-Poulsen, Adv. Sci. **6**, 1900367 (2019).
[22] M. Mansø, A. U. Petersen, Z. H. Wang, P. Erhart, M. B. Nielsen, and K. Moth-Poulsen, Nat. Commun. **9**, 1945 (2018).
[23] A. Cuppoletti, J. P. Dinnocenzo, J. L. Goodman, and I. R. Gould, J. Phys. Chem. A **103**, 11253 (1999).
[24] V. A. Bren, A. D. Dubonosov, V. I. Minkin, and V. A. Chernoivanov, Russ. Chem. Rev. **60**, 451 (1991).
[25] O. Brummel, F. Waidhas, U. Bauer, Y. L. Wu, S. Bochmann, H. P. Steinrück, C. Papp, J. Bachmann, and J. Libuda, J. Phys. Chem. Lett. **8**, 2819 (2017).
[26] M. Quant, A. Lennartson, A. Dreos, M. Kuisma, P. Erhart, K. Borjesson, and K. Moth-Poulsen, Chem.—Eur. J. **22**, 13265 (2016).
[27] M. Jevric, A. U. Petersen, M. Mansø, S. K. Singh, Z. H. Wang, A. Dreos, C. Sumby, M. B. Nielsen, K. Borjesson, P. Erhart, and K. Moth-Poulsen, Chem.—Eur. J. **24**, 12767 (2018).
[28] M. Jevric, Z. H. Wang, A. U. Petersen, M. Mansø, C. J. Sumby, M. B. Nielsen, and K. Moth-Poulsen, Eur. J. Org. Chem. **13**, 2354 (2019).
[29] R. W. Hoffmann and W. Barth, J. Chem. Soc., Chem. Commun. **7**, 345 (1983).
[30] G. F. Koser and J. N. Faircloth, J. Org. Chem. **41**, 583 (1976).
[31] K. Maruyama and H. Tamiaki, J. Org. Chem. **51**, 602 (1986).
[32] U. Bauer, L. Fromm, C. Weiß, P. Bachmann, F. Späth, F. Düll, J. Steinhauer, W. Hieringer, A. Görling, A. Hirsch, H. P. Steinrück, and C. Papp, J. Phys. Chem. C **123**, 7654 (2018).
[33] O. Brummel, D. Besold, T. Döpper, Y. L. Wu, S. Bochmann, F. Lazzari, F. Waidhas, U. Bauer, P. Bachmann, C. Papp, H. P. Steinrück, A. Görling, J. Libuda, and J. Bachmann, Chemsuschem **9**, 1424 (2016).
[34] F. Waidhas, M. Jevric, L. Fromm, M. Bertram, A. Görling, K. Moth-Poulsen, O. Brummel, and J. Libuda, Nano Energy **63**, 103872 (2019).
[35] M. Grätzel, J. Photochem. Photobiol., C **4**, 145 (2003).
[36] C. Schuschke, M. Schwarz, C. Hohner, T. N. Silva, L. Fromm, T. Döpper, A. Görling, and J. Libuda, J. Phys. Chem. Lett. **9**, 1937 (2018).
[37] M. Schwarz, S. Mohr, T. Xu, T. Döpper, C. Weiß, K. Civale, A. Hirsch, A. Görling, and J. Libuda, J. Phys. Chem. C **121**, 11508 (2017).
[38] M. Bertram, C. Schuschke, F. Waidhas, M. Schwarz, C. Hohner, M. Montero, O. Brummel, and J. Libuda, Phys. Chem. Chem. Phys. **21**, 23364 (2019).
[39] C. Schuschke, C. Hohner, M. Jevric, A. U. Petersen, Z. H. Wang, M. Schwarz, M. Kettner, F. Waidhas, L. Fromm, C. J. Sumby, A. Görling, O. Brummel, K. Moth-Poulsen, and J. Libuda, Nat. Commun. **10**, 2384 (2019).
[40] W. Meyer, K. Biedermann, M. Gubo, L. Hammer, and K. Heinz, J. Phys.: Condens. Matter **20**, 265011 (2008).
[41] F. Faisal, M. Bertram, C. Stumm, F. Waidhas, O. Brummel, and J. Libuda, Rev. Sci. Instrum. **89**, 114101 (2018).
[42] K. Biedermann, M. Gubo, L. Hammer, and K. Heinz, J. Phys.: Condens. Matter **21**, 185003 (2009).
[43] F. Faisal, C. Stumm, M. Bertram, F. Waidhas, Y. Lykhach, S. Cherevko, F. F. Xiang, M. Ammom, M. Vorokhta, B. Smid, T. Skala, N. Tsud, A. Neitzel, K. Beranova, K. C. Prince, S. Geiger, O. Kasian, T. Wähler, R. Schuster, M. A. Schneider, V. Matolin, K. J. J. Mayrhofer, O. Brummel, and J. Libuda, Nat. Mater. **17**, 592 (2018).

[44]TURBOMOLE, University of Karlsruhe, Forschungszentrum Karlsruhe GmbH, 2013.
[45]J. P. Perdew, K. Burke, and M. Ernzerhof, Phys. Rev. Lett. **77**, 3865 (1996).
[46]F. Weigend and R. Ahlrichs, Phys. Chem. Chem. Phys. **7**, 3297 (2005).
[47]S. Grimme, J. Antony, S. Ehrlich, and H. Krieg, J. Chem. Phys. **132**, 154104 (2010).
[48]S. Grimme, S. Ehrlich, and L. Goerigk, J. Comput. Chem. **32**, 1456 (2011).
[49]F. Weigend, Phys. Chem. Chem. Phys. **8**, 1057 (2006).
[50]M. Chen, R. Guo, Y. Zhao, S. F. Weng, Y. Z. Xu, I. Noda, and J. G. Wu, J. Mol. Struct. **1124**, 244 (2016).
[51]T. Iwasita and F. C. Nart, Prog. Surf. Sci. **55**, 271 (1997).